Int. J. Solids Structures Vol. 22, No. 5, pp. 467–483, 1986
Printed in Great Britain.

0020–7683/86 $3.00 + .00
Pergamon Journals Ltd.

NONLINEAR AXISYMMETRIC STATIC AND TRANSIENT ANALYSIS OF ORTHOTROPIC THIN TAPERED ANNULAR PLATES

P. C. DUMIR and K. N. KHATRI
Department of Applied Mechanics, Indian Institute of Technology, New Delhi-110016, India

(*Received* 24 *January* 1984; *in revised form* 17 *September* 1984)

Abstract—This paper considers the geometrically nonlinear axisymmetric static and transient responses of cylindrically orthotropic thin tapered annular plates subjected to uniformly distributed and ring loads. Immovable clamped and simply supported annular tapered plates with and without a rigid plug subjected to static and step function loads have been analysed. Orthogonal point collocation method and Newmark-β scheme have been employed to solve nonlinear governing differential equations expressed in terms of transverse displacement ω and stress function Ψ. Results have been presented for isotropic and orthotropic annular tapered plates with linear variation of thickness for two annular ratios and three taper ratios, and the effect of varying thickness has been investigated. A simple approximate method has been used to predict the maximum dynamic response to step loads from the results for static loads. This method gives sufficiently accurate results for engineering applications.

NOTATION

a, b	Outer and inner radii of the annulus
r, θ, z	Cylindrical coordinates of a material point
H_0, h_0, h	Thicknesses at centre ($r = 0$) at inner radius ($r = b$), and at radius r
$E_\theta, E_r; \nu_\theta, \nu_r$	Elastic moduli, Poisson's ratios
β	Orthotropic parameter $= E_\theta/E_r = \nu_\theta/\nu_r$
γ, α	Mass density, taper ratio
q, p	Intensity of distributed load, ring load at hole
Q, P	Nondimensional loads: $qa^4/E_r h_0^4$, $pa^2/E_r h_0^2$
ξ, M^*	$b/(a-b)$, central rigid mass
ρ, M	Nondimensional radius $(r-b)/(a-b)$, nondimensional mass $M^*/(\gamma\pi b^2 h_0)$
D, D_0	$E_\theta h^3/12(\beta - \nu_\theta^2)$, $E_\theta h_0^3/12(\beta - \nu_\theta^2)$
t, τ	Time, nondimensional time $[D_0/\gamma h_0 a^4]^{1/2} t$
$U(Q), U(P)$	Strain energy of plate for static loads Q and P
$\omega^*, u^*; \Psi^*$	Transverse and inplane displacements; stress function
$\omega, u; \Psi$	Nondimensional displacements and stress function
$\sigma_{r,\theta}; \epsilon_{r,\theta}$	Stresses and strains
$N_r, N_\theta; Q_r$	Inplane stress resultants; transverse shear force
M_r, M_θ	Moment stress resultants
$(\ )_{,r}; (\ )_{,t}$	Partial derivatives w.r.t. r and t
$(\ )', (\dot{})$	Partial derivatives w.r.t. ρ and τ
$\Delta\tau; \Delta Q, \Delta P$	Time and load increments
$p_0, P_0; q_0, Q_0$	Step loads
N, ρ_i	Number and radii of collocation points
a_i, b_i	Coefficients in the expansion of ω and Ψ
A_1, A_2, A_3	Coefficients of quadratic extrapolation
$(\ )_j, (\ )_i$	Values of jth step and at ith collocation point
$(\ )_p$	Predicted value

1. INTRODUCTION

Annular plates of variable thicknesses are often encountered in the design of various components such as diaphragms of steam turbines, piston heads, cylinder heads and coupling for power transmission shafts. With the increasing use of fibre-reinforced composite plates, it is of interest to study the static and transient nonlinear responses of orthotropic thin tapered annular plates. Murthy and Sherbourne[1] and Turvey[2] employed dynamic relaxation techniques to study the static axisymmetric nonlinear response of isotropic circular and annular plates of varying thicknesses, respectively. Static response of tapered annular isotropic plates under uniformly distributed load

SAS 22:5-A

was obtained by Tielking[3] using the Ritz method. Nonlinear axisymmetric bending of polar orthotropic annular plates of varying thicknesses has been studied by Reddy and Huang[4] using finite elements. Axisymmetric large-amplitude free vibrations of thick orthotropic annular plates of varying thicknesses have been analysed by Reddy and Huang[5] using finite elements. Transient response of clamped and simply supported orthotropic uniform thin annular plates, resting on Pasternak foundations, subjected to uniformly distributed step loads, has been presented by Nath and Jain[6] using Chebyshev series and the Houbolt scheme. Transient response of orthotropic or isotropic tapered annular plates has not been reported.

The objective of this investigation is to obtain the geometrically nonlinear axisymmetric static and transient response of cylindrically orthotropic thin tapered annular plates subjected to uniformly distributed and ring loads. The moderately large response of clamped and simply supported annular plates with and without a rigid plug has been obtained for static and step function loads. Dynamic analogues of von Kármán equations for orthotropic circular plates of varying thicknesses have been employed. An approximate value of the maximum central response under step loads has also been obtained from the response for static loads. The effect of edge conditions, taper ratio and orthotropic parameter on the response has been determined.

Nonlinear governing differential equations in terms of transverse displacement ω and stress function Ψ have been employed. Polynomial expansions are used for ω and Ψ, and the differential equations are discretised spacewise by the orthogonal point collocation method[7] with the zeros of a Legendre polynomial as collocation points. The Newmark-β scheme[8] is used for time-marching. At each step of the marching parameter, load or time, the nonlinear equations are solved iteratively. One of the factors in the product terms constituting the nonlinearity is predicted as the mean of its value at the two preceding iterations. For the first iteration, the predicted value is extrapolated quadratically from the values at the three preceding steps.

2. GOVERNING EQUATIONS

The strain–displacement relations for moderately large axisymmetric deflection and the stress–strain relations for cylindrically orthotropic elastic material are

$$\epsilon_r = u^*_{,r} + \frac{1}{2}\omega^{*2}_{,r} - z\omega^*_{,rr} = \frac{\sigma^*_r}{E_r} - \nu_\theta \frac{\sigma^*_\theta}{E_\theta}, \tag{1}$$

$$\epsilon_\theta = \frac{u^* - z\omega^*_{,r}}{r} = \frac{\sigma^*_\theta}{E_\theta} - \nu_r \frac{\sigma^*_r}{E_r}, \tag{2}$$

with $\beta = E_\theta/E_r = \nu_\theta/\nu_r$. The stress resultants are related to displacements by

$$N_r = \int_{-h/2}^{h/2} \sigma^*_r \, dz = \frac{E_\theta h}{\beta - \nu_\theta^2}\left[u^*_{,r} + \frac{1}{2}\omega^{*2}_{,r} + \frac{\nu_\theta u^*}{r}\right],$$
$$N_\theta = \int_{-h/2}^{h/2} \sigma^*_\theta \, dz = \frac{E_\theta h}{\beta - \nu_\theta^2}\left[\nu_\theta\left(u^*_{,r} + \frac{1}{2}\omega^{*2}_{,r}\right) + \frac{\beta u^*}{r}\right]; \tag{3}$$

$$M_r = \int_{-h/2}^{h/2} z\sigma^*_r \, dz = -D\left(\omega^*_{,rr} + \frac{\nu_\theta \omega^*_{,r}}{r}\right),$$
$$M_\theta = \int_{-h/2}^{h/2} z\sigma^*_\theta \, dz = -D\left(\nu_\theta \omega^*_{,rr} + \frac{\beta \omega^*_{,r}}{r}\right); \tag{4}$$

$$Q_r = \int_{-h/2}^{h/2} \sigma^*_{rz} \, dz, \tag{5}$$

where $D = E_\theta h^3/[12(\beta - \nu_\theta^2)]$ is the flexural rigidity.

Neglecting inplane inertia, rotary inertia and damping, Hamilton's principle yields the differential equations and the boundary conditions as

$$(rN_r)_{,r} - N_\theta = 0, \tag{6}$$

$$M_{\theta,r} - (rM_r)_{,rr} - (rN_r\omega^*_{,r})_{,r} = (q - \gamma h\omega^*_{,tt})r \tag{7}$$

and prescribed values at the boundaries for

$$N_r \text{ or } u^*, \qquad M_r \text{ or } \omega^*_{,r}, \qquad rQ_r = (rM_r)_{,r} - M_\theta + rN_r\omega^*_{,r} \text{ or } \omega^*. \tag{8}$$

Integrating (7) from the inner radius b to r (Fig. 1) and using the shear boundary condition at the inner boundary give

$$M_\theta - (rM_r)_{,r} - rN_r\omega^*_{,r} = \frac{p}{2\pi} + \int_b^r (q - \gamma h\omega^*_{,tt})r\,dr, \tag{9}$$

where p is the total ring load at the hole and q is the intensity of the distributed load. Equation (6) is satisfied in terms of a stress function Ψ^* with

$$N_r = \Psi^*/r, \qquad N_\theta = \Psi^*_{,r}. \tag{10}$$

The compatibility equation for strains at the midplane can be expressed in terms of stress function Ψ^* as

$$r^2\Psi^*_{,rr} + r\Psi^*_{,r} - \beta\Psi^* - \frac{rh_{,r}}{h}(r\Psi^*_{,r} - \nu_\theta\Psi^*) + \frac{1}{2}rhE_\theta\omega^{*2}_{,r} = 0. \tag{11}$$

Using eqns (4) and (10), eqn (9) can be written as

$$r^2\omega^*_{,rrr} + r\omega^*_{,rr} - \beta\omega^*_{,r} + \frac{D_{,r}}{D}(r^2\omega^*_{,rr} + \nu_\theta r\omega^*_{,r}) - \frac{r\Psi^*}{D}\omega^*_{,r}$$
$$= \frac{r}{D}\left[-\frac{bQ_r(b)}{2\pi} + \int_b^r (q - \gamma h\omega^*_{,tt})r\,dr\right] \tag{12}$$

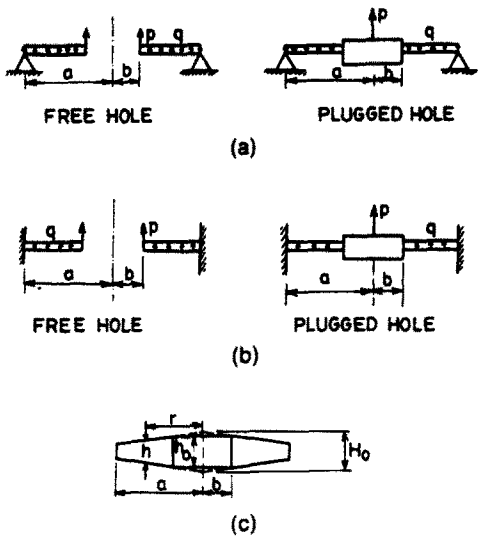

Fig. 1. Geometry and load on the annulus: (a) immovable simply supported annulus; (b) immovable clamped annulus; (c) thickness variation.

The equation of motion of the rigid central mass M^* is

$$M^*\omega^*_{,tt}(b) = p + 2\pi b Q_r(b). \tag{13}$$

Substituting $Q_r(b)$ from eqn (13) in eqn (12) reduces it to

$$r^2\omega^*_{,rrr} + r\omega^*_{,rr} - \beta\omega^*_{,r} + \frac{D_{,r}}{D}(r^2\omega^*_{,rr} + \nu_\theta r\omega^*_{,r}) - \frac{r\Psi^*}{D}\omega^*_{,r}$$
$$= \frac{r}{D}\left[-\frac{M^*}{2\pi}\omega^*_{,tt}(b) + \frac{p}{2\pi} + \int_b^r (q - \gamma h\omega^*_{,tt})r\,dr\right]. \tag{14}$$

Introducing the dimensionless parameters

$$\omega = \frac{\omega^*}{h_0}, \qquad \Psi = \frac{a-b}{D_0}\Psi^*, \qquad \xi = \frac{b}{a-b}, \qquad \rho = \frac{r-b}{a-b} \quad (0 \le \rho \le 1)$$
$$M = \frac{M^*}{\pi b^2 h_0 \gamma}, \qquad Q = \frac{qa^4}{E_r h_0^4}, \qquad P = \frac{pa^2}{E_r h_0^4}, \qquad \tau = \left[\frac{D_0}{\gamma h_0 a^4}\right]^{1/2} t, \tag{15}$$

the governing equations (14) and (11) reduce to the following dimensionless form:

$$(\rho+\xi)^2\omega''' + (\rho+\xi)\omega'' - \beta\omega' + \frac{D'}{D}[(\rho+\xi)^2\omega'' + \nu_\theta(\rho+\xi)\omega'] - \frac{D_0}{D}(\rho+\xi)\omega'\Psi$$
$$= \frac{D_0}{D}\frac{(\rho+\xi)}{(1+\xi)^4}\left[-\frac{\xi^2}{2}M\ddot{\omega}(0) + \frac{6(\beta-\nu_\theta^2)}{\pi\beta}(1+\xi)^2 P\right.$$
$$\left. + \int_0^\rho \left\{\frac{12(\beta-\nu_\theta^2)}{\beta}Q - \frac{h}{h_0}\ddot{\omega}\right\}(\rho+\xi)\,d\rho\right], \tag{16}$$

$$(\rho+\xi)^2\Psi'' + (\rho+\xi)\Psi' - \beta\Psi - (\rho+\xi)\frac{h'}{h}\{(\rho+\xi)\Psi' - \nu_\theta\Psi\}$$
$$+ 6(\beta-\nu_\theta^2)(\rho+\xi)\frac{h}{h_0}\omega'^2 = 0, \tag{17}$$

where $(\,)'$ and $(\dot{})$ are derivatives w.r.t ρ and τ, respectively, and h_0, D_0 are the thickness and flexural rigidity of the plate at $\rho = 0$ ($r = b$).

$$D_0 \equiv E_\theta h_0^3/[12(\beta - \nu_\theta^2)]. \tag{18}$$

The initial conditions are assumed as

$$\omega(\rho, 0) = \dot{\omega}(\rho, 0) = 0. \tag{19}$$

The boundary conditions for clamped and simply supported annulus with free and plugged holes (Fig. 1) are

$\rho = 0$:

$$\omega''(0) + \nu_\theta\omega'(0)/\xi = 0, \quad \Psi(0) = 0 \qquad \text{(free hole)}, \tag{20a}$$
$$\omega'(0) = 0, \quad \Psi'(0) - \nu_\theta\Psi(0)/\xi = 0 \qquad \text{(plugged hole)}; \tag{20b}$$

$\rho = 1$:

$$\omega(1) = 0, \quad \Psi'(1) - \nu_\theta \Psi(0)/(1 + \xi) = 0, \tag{21}$$

$$\omega'(1) = 0 \quad \text{(clamped edge)}, \tag{22a}$$

$$\omega''(1) + \nu_\theta \omega'(1)/(1 + \xi) = 0 \quad \text{(simply supported edge)}. \tag{22b}$$

Results have been presented for the case of linear variation of thickness

$$h = H_0(1 + \alpha r/a) = h_0[(1 + \xi) + \alpha(\rho + \xi)]/[(1 + \xi) + \alpha\xi], \tag{23}$$

where H_0, h_0 are the thicknesses at the centre and hole, and α is the taper ratio.

3. METHOD OF SOLUTION

The load or time is incremented in small steps for the static and dynamic cases, respectively. The nonlinear equations (16) and (17) are solved iteratively at each step J by linearising the nonlinear terms as

$$(\omega'\Psi)_J = \omega'_{J_p} \Psi_J, \qquad (\omega')^2_J = \omega'_{J_p} \omega'_J, \tag{24}$$

where, the predicted term ω'_{J_p} is taken as the mean of its value at the two preceding iterations. For the first iteration, the predicted value ω'_{J_p} is extrapolated quadratically from the values of ω' at the three preceding steps as follows:

$$\omega'_{J_p} = A_1\omega'_{J-1} + A_2\omega'_{J-2} + A_3\omega'_{J-3}, \tag{25}$$

where A_1, A_2, A_3 for various steps are: 1, 0, 0 ($J = 1$); 2, -1, 1 ($J = 2$); 3, -3, 1 ($J \geq 3$).

The orthogonal point collocation method, with zeros of a Legendre polynomial as collocation points, has been used to solve eqns (16) and (17). For N collocation points, the deflection and stress functions are expanded as polynomials in the dimensionless radius ρ:

$$\omega(\rho) = \sum_{m=1}^{N+3} \rho^{m-1} a_m, \quad \Psi(\rho) = \sum_{n=1}^{N+2} \rho^{n-1} b_n, \qquad 0 \leq \rho \leq 1. \tag{26}$$

Table 1. Convergence study for uniformly distributed step load on clamped plate with free hole

[$\beta = 3$, $\gamma_\theta = 0.3$, $\frac{b}{a} = 0.25$, $\alpha = -\frac{1}{3}$, $Q_0 = 10$]

N	$\Delta\tau$	τ	$\omega(0)$	$\omega(0)_{max}$	τ	τ	W(0)
			TEMPORAL CONVERGENCE ($N = 6$)				
6	0.001	0.120	1.208	1.620	at 0.168	0.240	1.235
6	0.002	0.120	1.209	1.623	at 0.164	0.240	1.235
6	0.003	0.120	1.208	1.623	at 0.171	0.240	1.237
6	0.004	0.120	1.211	1.621	at 0.176	0.240	1.237
6	0.005	0.120	1.220	1.618	at 0.155	0.240	1.227
			SPATIAL CONVERGENCE ($\Delta\tau = 0.002$)				
5	0.002	0.120	1.206	1.627	at 0.162	0.240	1.225
6	0.002	0.120	1.209	1.623	at 0.164	0.240	1.235
7	0.002	0.120	1.212	1.622	at 0.164	0.240	1.235

The N collocation points ρ_i are taken at the zeros of an Nth degree Legendre polynomial in the range 0 to 1. The Newmark-β scheme with parameters corresponding to the average acceleration method is used to discretise the inertia term:

$$\begin{aligned}
\dot{\omega}_J &= \dot{\omega}_{J-1} + \tfrac{1}{2}(\ddot{\omega}_{J-1} + \ddot{\omega}_J)\,(\Delta\tau),\\
\omega_J &= \omega_{J-1} + \dot{\omega}_{J-1}(\Delta\tau) + \tfrac{1}{4}(\ddot{\omega}_{J-1} + \ddot{\omega}_J)\,(\Delta\tau)^2,\\
\ddot{\omega}_J &= 4(\omega_J - \omega_{J-1})/(\Delta\tau)^2 - 4\dot{\omega}_{J-1}/(\Delta\tau) - \ddot{\omega}_{J-1}.
\end{aligned} \tag{27}$$

The $2N$ collocation equations for the differential equations (16) and (17) are

$$\begin{aligned}
&\sum_{m=1}^{N+3}\Bigg[(m-1)\Bigg\{(\rho_i+\xi)^2(m-2)(m-3)\rho_i^{m-4} + (\rho_i+\xi)(m-2)\rho_i^{m-3} - \beta\rho_i^{m-2}\\
&\quad + 3\left(\frac{h'}{h}\right)_i(\rho_i+\xi)\left((m-2)(\rho_i+\xi)+\nu_\theta\right)\Bigg\}\\
&\quad + \frac{4}{(\Delta\tau)^2}\frac{\rho_i+\xi}{(1+\xi)^4}\left(\frac{h_0}{h_i}\right)^3\left\{\int_0^{\rho_i}\left(\frac{h}{h_0}\right)(\rho^m + \xi\rho^{m-1})\,d\rho\right\}\Bigg]a_m\\
&\quad + \frac{2}{(\Delta\tau)^2}\frac{\rho_i+\xi}{(1+\xi)^4}\left(\frac{h_0}{h_i}\right)^3\xi^2 M a_1 - \sum_{n=1}^{N+2}\left[(\rho_i+\xi)(\omega'_{J_n})_i\left(\frac{h_0}{h}\right)_i^3\rho_i^{n-1}\right]b_n\\
&= \frac{\rho_i+\xi}{(1+\xi)^4}\left(\frac{h_0}{h_i}\right)^3\Bigg[\frac{6(\beta-\nu_\theta^2)}{\pi\beta}(1+\xi)^2 P_J\\
&\quad + \int_0^{\rho_i}\left\{\frac{12(\beta-\nu_\theta^2)}{\beta}Q_J + \frac{h}{h_0}\left(\frac{4\omega}{(\Delta\tau)^2} + \frac{4\dot{\omega}}{(\Delta\tau)} + \ddot{\omega}\right)_{J-1}\right\}(\rho+\xi)\,d\rho\\
&\quad + \frac{\xi^2}{2}M\left\{\frac{4\omega(0)}{(\Delta\tau)^2} + \frac{4\dot{\omega}(0)}{(\Delta\tau)} + \ddot{\omega}(0)\right\}_{J-1}\Bigg],
\end{aligned} \tag{28}$$

$$\begin{aligned}
&\sum_{m=1}^{N+3}\left[6(\beta-\nu_\theta^2)(m-1)(\rho_i+\xi)(\omega'_{J_n})_i\left(\frac{h}{h_0}\right)_i\rho_i^{m-2}\right]a_m\\
&\quad + \sum_{n=1}^{N+2}\Bigg[(\rho_i+\xi)^2(n-1)(n-2)\rho_i^{n-3}\\
&\quad + (\rho_i+\xi)\Bigg\{(n-1)\rho_i^{n-2} - \beta\rho_i^{n-1}\\
&\quad - \left(\frac{h'}{h}\right)_i\left((\rho_i+\xi)(n-1)\rho_i^{n-2} - \nu_\theta\rho_i^{n-1}\right)\Bigg\}\Bigg]b_n = 0,
\end{aligned}$$

$$i = 1, 2, \ldots, N. \tag{29}$$

The five equations for the boundary conditions are solved for a_1, a_2, a_3 and b_1, b_2 in terms of the remaining N as and N bs, respectively. Equations (28) and (29) are the $2N$ discretised equations for these as and bs. These are solved by Gaussian elimination with pivoting. The iterations are continued until $\omega(0)$, $\Psi'(0)$ and $\Psi'(1)$ converge within 0.1% accuracy. The sum of the kinetic and strain energies of the plate at each step is compared with the sum of the initial kinetic energy and the work done up to that step. The balance of energy is found to have been maintained very well at each step, thus ensuring accuracy of the results. Timewise and spacewise convergence studies have established that six collocation points and $\Delta\tau = 0.002$ are sufficient to yield accurate converged results. Typical results of a convergence study for a clamped orthotropic tapered plate with a free hole under uniformly distributed step load are given in Table 1.

4. APPROXIMATE MAXIMUM RESPONSE FOR STEP LOADS

The approximate value of the maximum response $\omega(0)_{max}$ under step loads has been obtained from static response. It is based on the assumptions that at the instant of the maximum deflection at the hole, the annulus has zero velocity, and the deflected shape $\omega^*(r)$ is the same as that under a static load which causes the same deflection at the hole. If the static uniformly distributed load Q results in a deflection $\omega(0)$ with the strain energy $U(Q)$, then the step load Q_0 which will yield the maximum deflection $\omega(0)_{max}$ equal to $\omega(0)$ is given by

$$\int_a^b \omega^*(r) q_0 2\pi r \, dr = 2\pi E_r \frac{h_0^5}{a^2} Q_0 \left[\sum_{m=1}^{N+3} \left(\frac{1}{m+1} + \frac{\xi}{m}\right) a_m\right] = U(Q),$$
$$Q_0 = \frac{a^2 U(Q)}{2\pi E_r h_0^5} \Big/ \left[\sum_{m=1}^{N+3} \left(\frac{1}{m+1} + \frac{\xi}{m}\right) a_m\right]. \tag{30}$$

Similarly, if the static central load P causes deflection $\omega(0)$ with the strain energy $U(P)$, then the central step load P_0 at the hole which will yield the maximum deflection $\omega(0)_{max}$ equal to $\omega(0)$ is given by

$$P_0 = \frac{a^2 U(P)}{E_r h_0^5 \omega(0)} = \frac{a^2 U(P)}{E_r h_0^5 a_1}. \tag{31}$$

5. RESULTS AND DISCUSSION

Transient response of isotropic and orthotropic thin annular plates with linear variation of thickness has been obtained for uniformly distributed and central ring loads

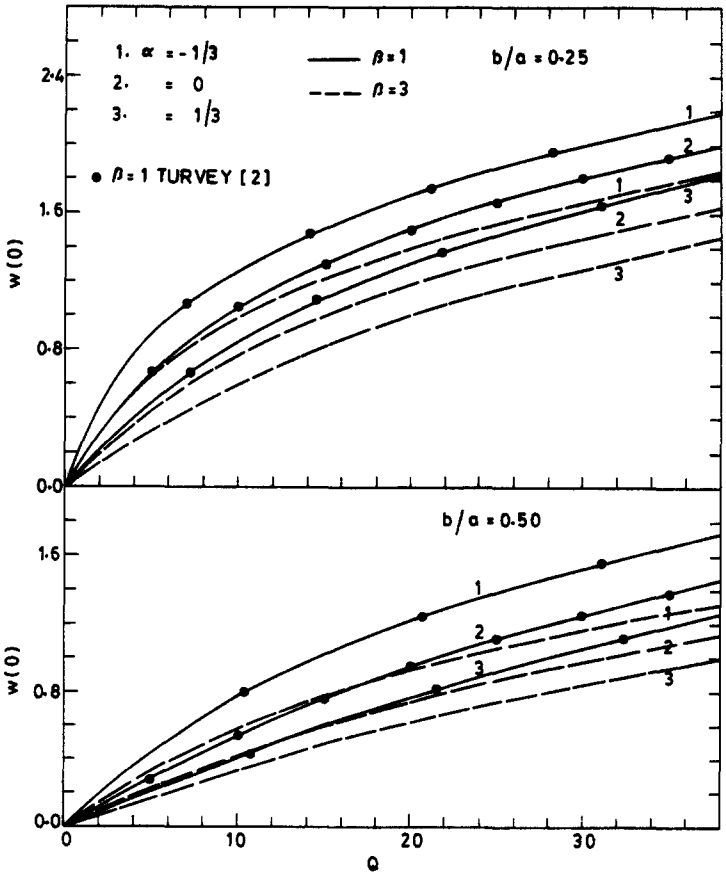

Fig. 2. Deflection for clamped plate with free hole under uniformly distributed static load.

Table 2. Maximum deflection under step loads

			Free hole						Plugged hole (M = 2)					
			Q_0 = 10			P_0 = 10			Q_0 = 15			P_0 = 15		
β	α	b/a	$\omega(0)_{max}$	Approx. $\omega(0)_{max}$	Error %	$\omega(0)_{max}$	Approx. $\omega(0)_{max}$	Error %	$\omega(0)_{max}$	Approx. $\omega(0)_{max}$	Error %	$\omega(0)_{max}$	Approx. $\omega(0)_{max}$	Error %
							CLAMPED PLATE							
1	−1/3	0.25	1.993	1.993	0.0	2.334	2.400	2.8	1.804	1.777	−1.5	1.825	1.833	0.4
	0		1.698	1.715	1.0	2.081	2.123	2.0	1.548	1.508	−2.6	1.560	1.580	1.3
	1/3		1.494	1.466	−1.8	1.848	1.887	2.1	1.343	1.289	−4.0	1.351	1.380	2.1
3	−1/3	0.25	1.623	1.630	0.4	1.825	1.874	2.7	1.768	1.736	−1.8	1.760	1.768	0.5
	0		1.335	1.330	−0.4	1.548	1.588	2.6	1.474	1.435	−2.7	1.466	1.485	1.3
	1/3		1.098	1.088	−0.9	1.333	1.364	2.4	1.239	1.194	−3.6	1.242	1.265	1.9
1	−1/3	0.50	1.385	1.367	−1.3	1.640	1.691	3.1	0.871	0.777	−10.8	0.836	0.779	−6.8
	0		1.021	1.017	−0.4	1.327	1.344	1.3	0.620	0.606	−2.3	0.625	0.628	0.5
	1/3		0.805	0.804	−0.2	1.102	1.114	1.1	0.460	0.504	−9.6	0.485	0.536	10.5
3	−1/3	0.50	1.076	1.039	−3.4	1.189	1.273	7.0	0.870	0.775	−10.9	0.834	0.775	−7.1
	0		0.821	0.800	−2.6	0.991	1.040	5.0	0.615	0.601	−2.3	0.618	0.621	0.5
	1/3		0.667	0.651	−2.4	0.848	0.885	4.3	0.454	0.499	10.0	0.478	0.529	10.7
							SIMPLY SUPPORTED PLATE							
1	−1/3	0.50	2.265	2.164	−4.4	2.346	2.346	0.0	1.266	1.203	−5.0	1.165	1.143	−1.9
	0		2.225	2.121	−4.7	2.264	2.283	0.9	1.176	1.149	−2.3	1.082	1.085	0.3
	1/3		2.182	2.086	−4.4	2.207	2.217	4.4	1.120	1.113	−0.6	1.019	1.047	2.8
3	−1/3	0.50	1.628	1.556	−4.4	1.687	1.689	0.1	1.257	1.191	−5.3	1.155	1.128	−2.4
	0		1.542	1.488	−3.5	1.597	1.598	0.1	1.147	1.122	−2.2	1.052	1.054	0.2
	1/3		1.488	1.435	−3.6	1.529	1.531	0.1	1.070	1.074	0.4	0.969	1.004	3.6

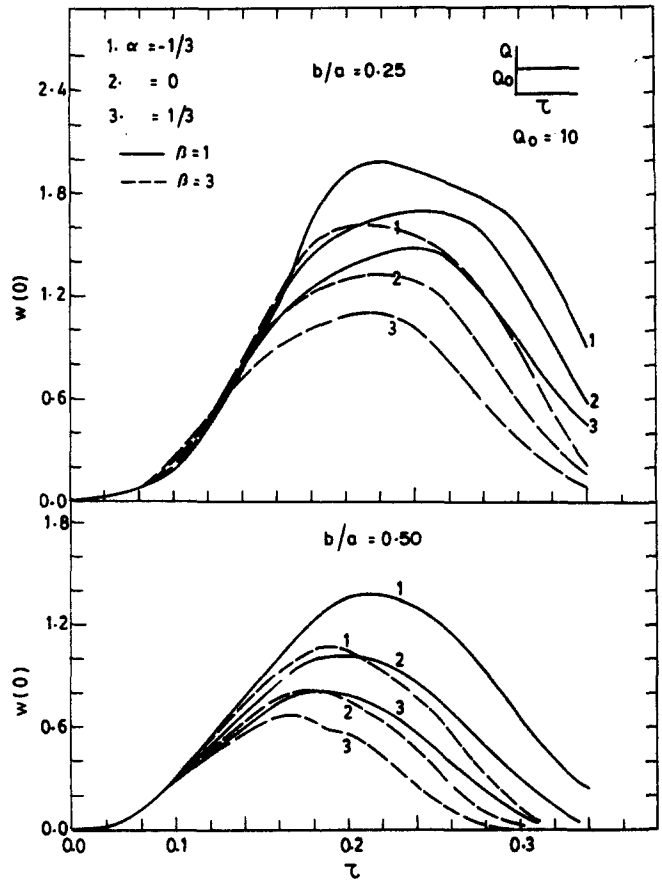

Fig. 3. Deflection response of clamped plate with free hole under uniformly distributed step load.

for two values of annular ratios and three taper ratios. Immovable clamped and simply supported annular plates with a free hole and a rigid plug have been analysed. Static analysis has also been presented from which approximate values of maximum response to step loads are obtained. Poisson's ratio ν_θ has been taken as 0.3.

The deflection response of isotropic ($\beta = 1$) and orthotropic ($\beta = 3$) clamped plate with a free hole under uniformly distributed static load is given in Fig. 2 for annular

Table 3. Maximum radial stress at support for clamped plates ($b/a = 0.25$) under step loads

β	α	σ^h_{max}	Approx. σ^h_{max}	Error %	σ^m_{max}	Approx. σ^m_{max}	Error %
			FREE HOLE $Q_0 = 10$				
1	−1/3	16.72	17.14	2.5	2.297	2.325	1.2
	0	11.89	12.08	1.6	1.251	1.258	0.6
	1/3	8.85	8.99	1.6	0.766	0.754	−1.6
3	−1/3	15.02	15.40	2.5	2.410	2.407	−0.1
	0	10.46	10.45	−0.1	1.198	1.197	−0.1
	1/3	7.74	7.72	−0.3	0.663	0.660	−0.5
			PLUGGED HOLE ($M = 2$) $Q_0 = 15$				
1	−1/3	20.94	22.13	5.7	3.660	3.617	−1.2
	0	14.93	15.59	4.4	2.072	2.045	−1.3
	1/3	11.61	11.91	2.6	1.316	1.285	−2.4
3	−1/3	19.63	20.90	6.5	3.622	3.595	−0.7
	0	13.87	14.55	4.9	1.916	1.921	0.3
	1/3	10.52	10.94	4.0	1.121	1.127	0.5

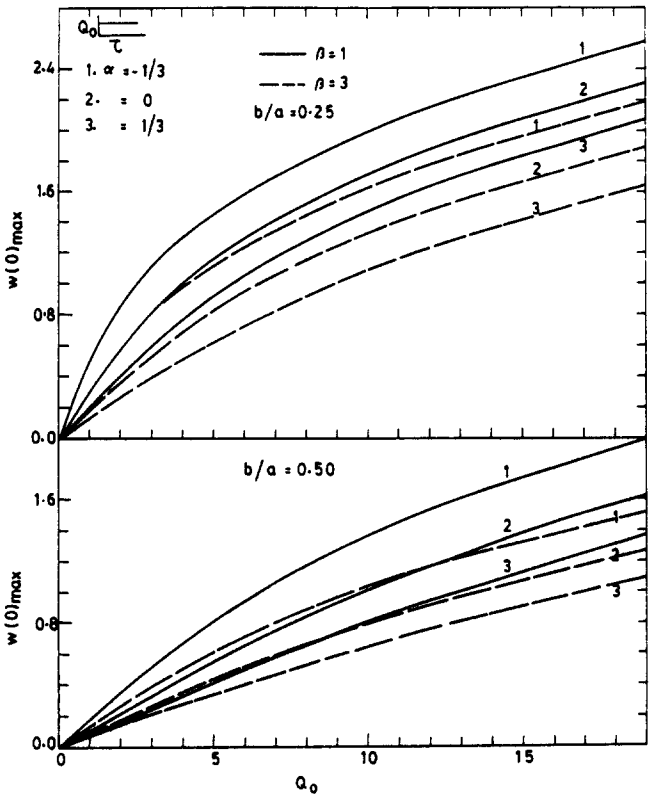

Fig. 4. Approximate $\omega(0)_{max}$ for clamped plate with free hole under uniformly distributed step load.

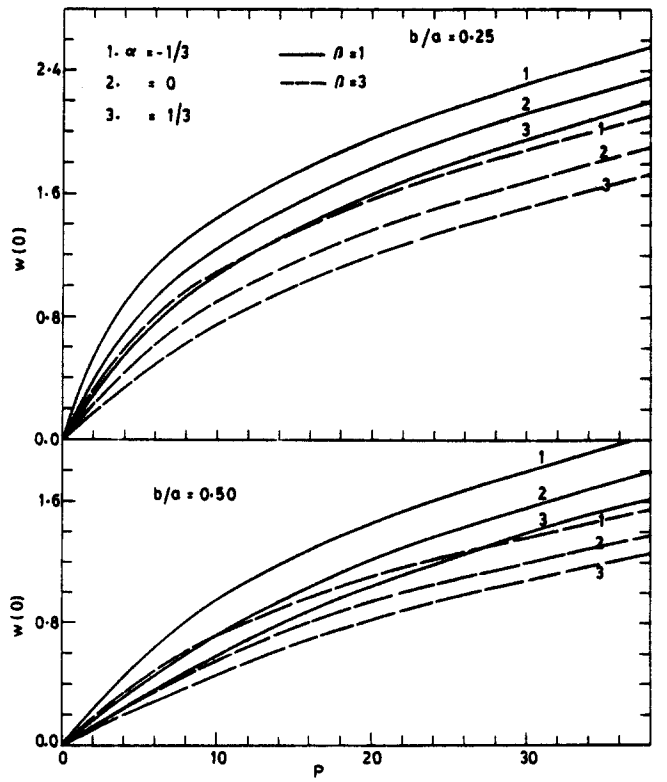

Fig. 5. Deflection for clamped plate with free hole under static ring load.

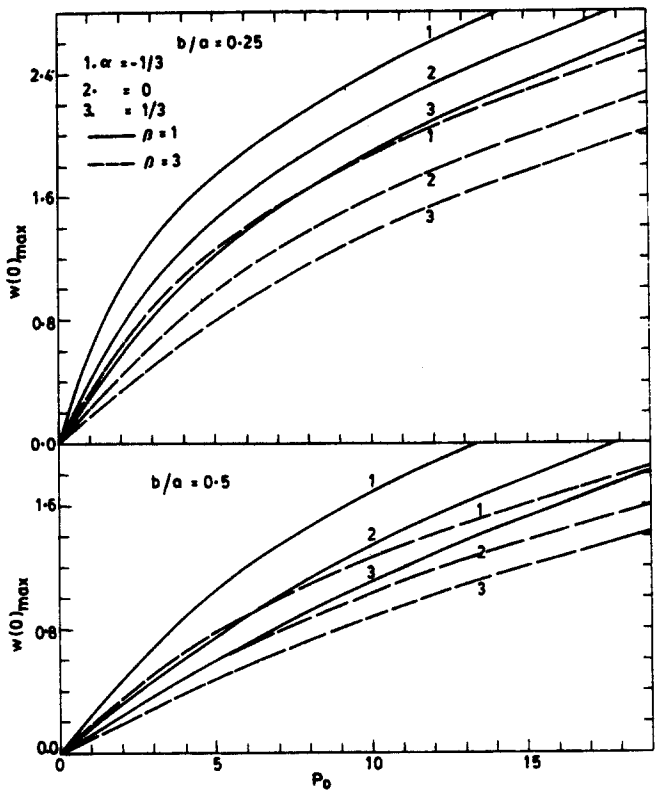

Fig. 6. Approximate $\omega(0)_{max}$ for clamped plate with free hole under step ring load.

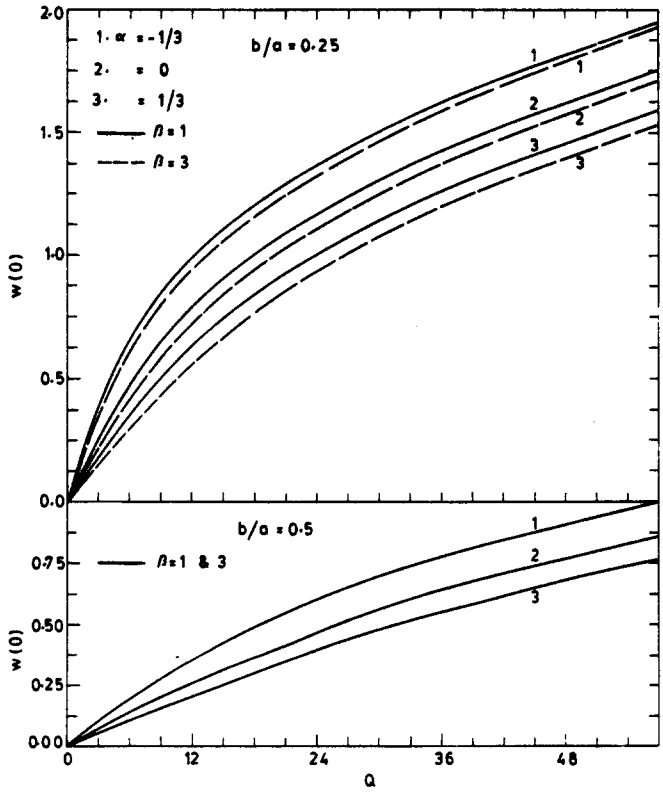

Fig. 7. Deflection for clamped plate with plugged hole under uniformly distributed static load.

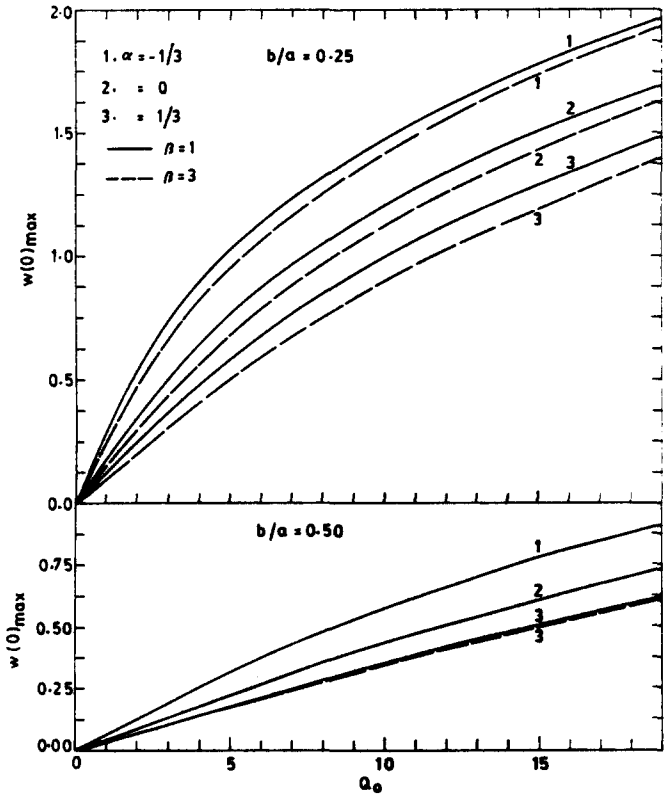

Fig. 8. Approximate $\omega(0)_{max}$ for clamped plate with plugged hole under uniformly distributed step load.

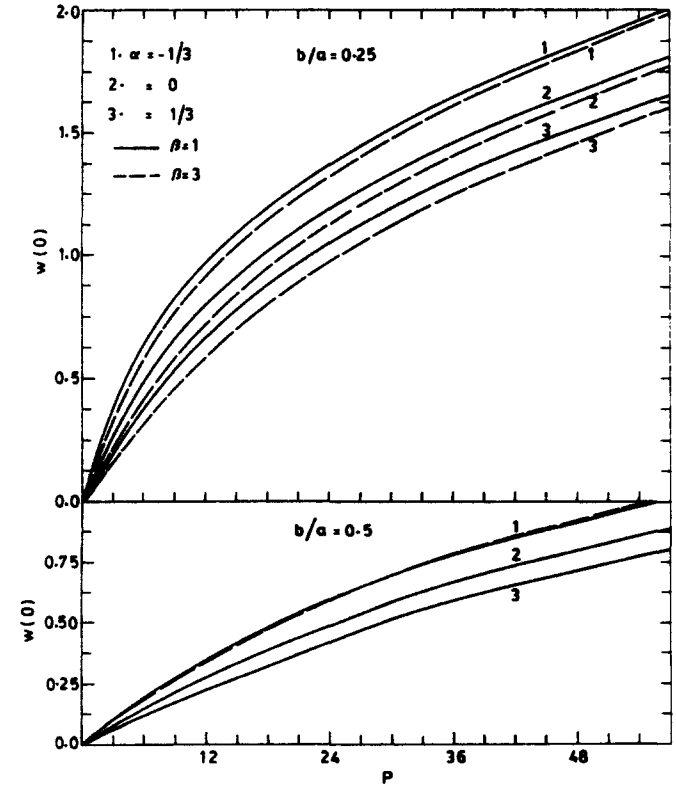

Fig. 9. Deflection for clamped plate with plugged hole under central static load.

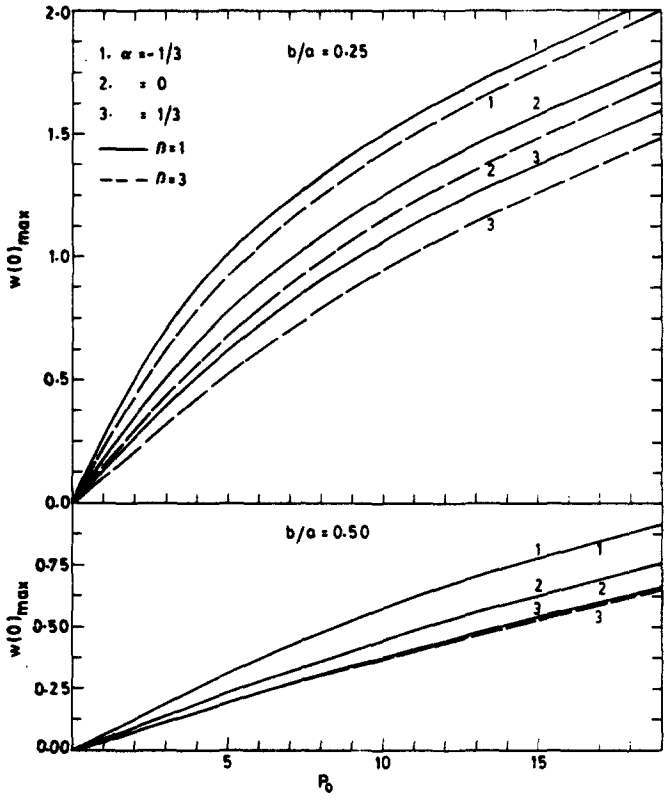

Fig. 10. Approximate $\omega(0)_{max}$ for clamped plate with plugged hole under central step load.

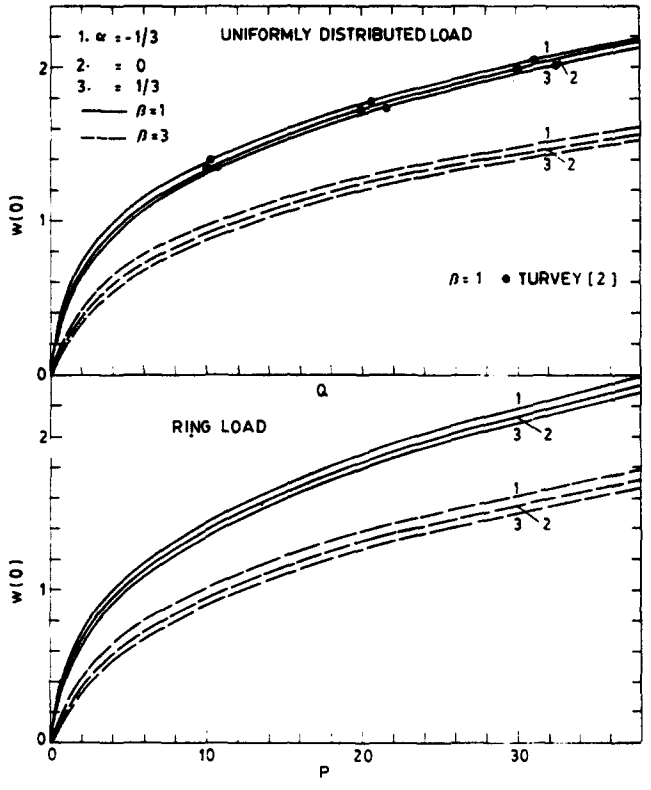

Fig. 11. Deflection for simply supported plate with free hole under static loads (b/a = 0.5).

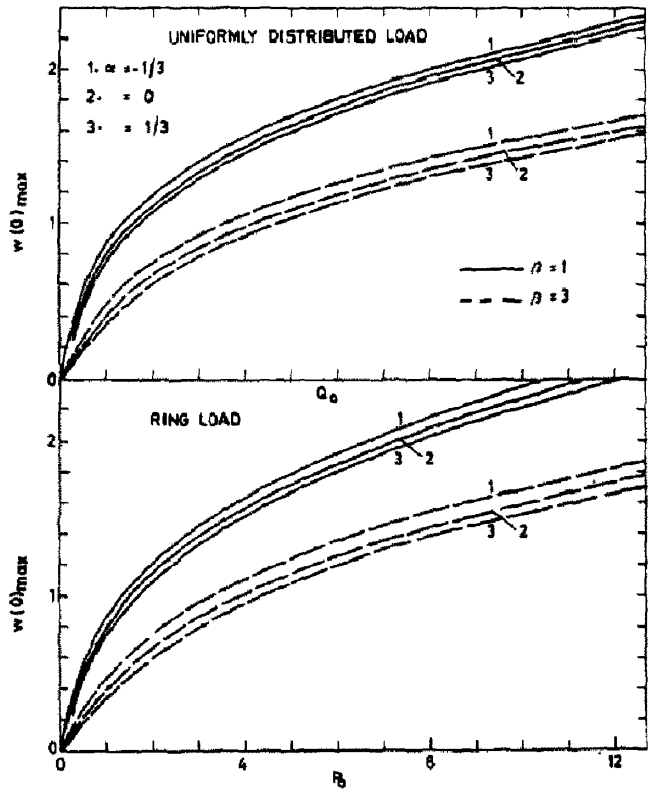

Fig. 12. Approximate $\omega(0)_{max}$ for simply supported plate with free hole under step loads (b/a = 0.5).

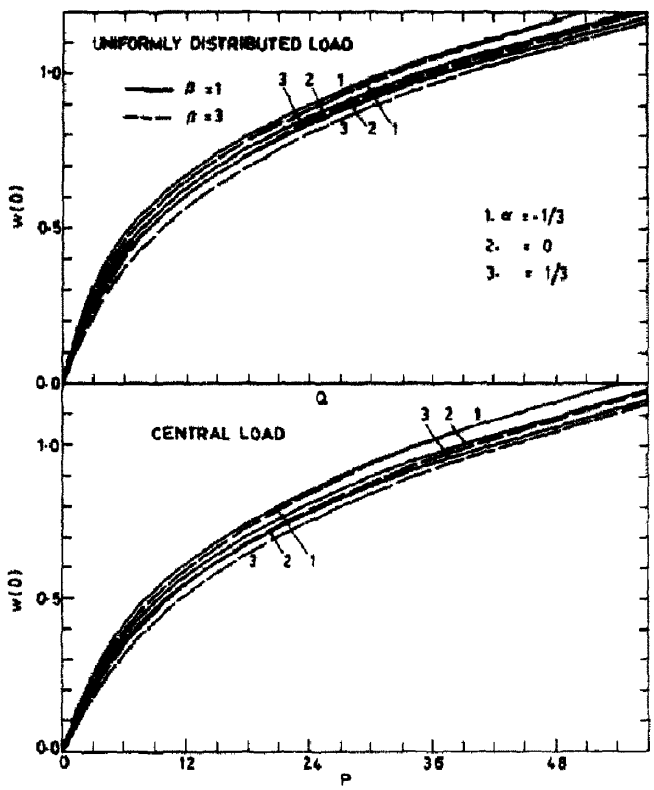

Fig. 13. Deflection for simply supported plate with plugged hole under static loads (b/a = 0.5).

ratios $b/a = 0.25, 0.5$ and taper ratios $\alpha = -1/3, 0, 1/3$. It can be seen from Fig. 2 that the present results for the isotropic case agree with those of Turvey[2], obtained by dynamic relaxation. The transient response of clamped plate with free hole under uniformly distributed step load $Q_0 = 10$ is shown in Fig. 3 for two values of β and b/a and three taper ratios. The maximum deflection $\omega(0)_{max}$ under step load $Q_0 = 10$ is given in Table 2 along with the approximate value of $\omega(0)_{max}$ calculated from the static response, as explained in Section 4. It is observed from Table 2 that for clamped plates with free hole under uniformly distributed step load, the error in the approximate values of $\omega(0)_{max}$ is less than 3.4%. The approximate values of $\omega(0)_{max}$ obtained from static results are depicted in Fig. 4 for a clamped plate with free hole under uniformly distributed load. The maximum deflection $\omega(0)_{max}$ under step loads obtained from dynamic analysis is compared in Table 2 with the approximate value of $\omega(0)_{max}$ obtained from static analysis using the method of Section 4. These results are presented for clamped and simply supported annular plates with and without rigid plugs under uniformly distributed step loads as well as ring loads at the hole for an orthotropic parameter $\beta = 1, 3$, annular ratio $b/a = 0.25, 0.50$ and taper ratio $\alpha = -1/3, 0, 1/3$. It is noted from Table 2 that the approximate method gives acceptable results for engineering applications, the error being less than 5% for most cases. The maximum error is 10.9%. The maximum radial bending and membrane stresses at the support are given in Table 3 for clamped plates, with $b/a = 0.25$, subjected to uniformly distributed loads. The values predicted from static analysis are also tabulated and are found to agree well with the results from the transient analysis. In view of the sufficiently accurate maximum response for step loads obtained from the static results, detailed static and approximate dynamic deflection responses for clamped plates with a free hole are plotted in Figs 5 and 6 for ring load at the hole. Static and dynamic deflection results for a clamped plate with plugged hole under uniformly distributed and ring loads are given

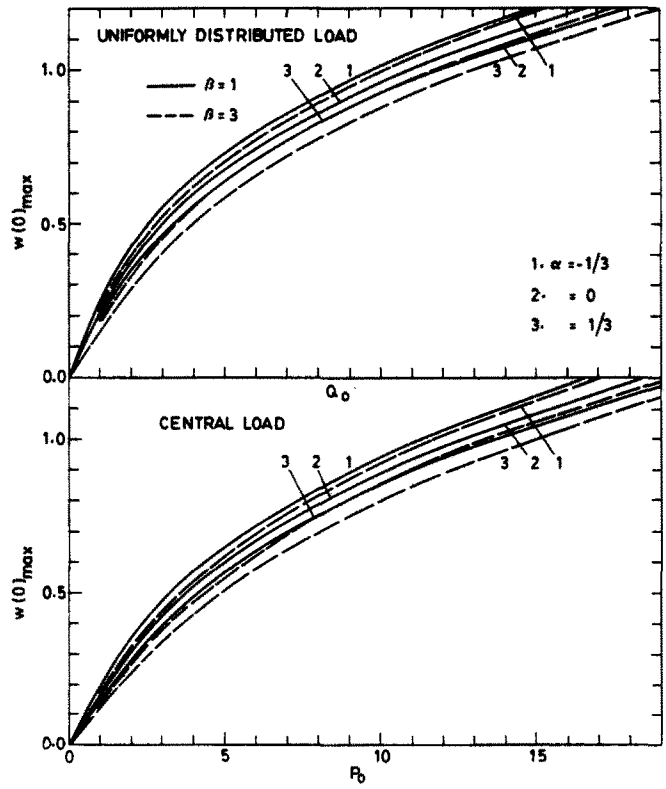

Fig. 14. Approximate $\omega(0)_{max}$ for simply supported plate with free hole under step loads ($b/a = 0.5$).

Table 4. Linear response under static load

β	α	b/a	ω(0)/Q for uniformly distributed load Q		ω(0)/P for ring/central load P	
			Free hole	Plugged hole	Free hole	Plugged hole
			CLAMPED PLATE			
1	−1/3	0.25	0.2850	0.1576	0.3486	0.1433
	0		0.1621	0.0927	0.2173	0.0923
	1/3		0.1085	0.0639	0.1546	0.0678
3	−1/3	0.25	0.1663	0.1321	0.1805	0.1172
	0		0.0984	0.0771	0.1195	0.0753
	1/3		0.0681	0.0530	0.0892	0.0553
1	−1/3	0.50	0.0928	0.0334	0.1250	0.0326
	0		0.0575	0.0230	0.0810	0.0238
	1/3		0.0428	0.0182	0.0619	0.0194
3	−1/3	0.50	0.0699	0.0327	0.0917	0.0319
	0		0.0459	0.0226	0.0633	0.0232
	1/3		0.0352	0.0179	0.0500	0.0190
			SIMPLY SUPPORTED PLATE			
1	−1/3	0.50	0.8805	0.1385	0.8630	0.1051
	0		0.6819	0.1128	0.6721	0.0877
	1/3		0.5696	0.0991	0.5633	0.0781
3	−1/3	0.50	0.3055	0.1200	0.2923	0.0910
	0		0.2317	0.0933	0.2252	0.0727
	1/3		0.1917	0.0793	0.1881	0.0628

in Figs 7, 8 and Figs 9, 10, respectively. Similar static and approximate dynamic results for a simply supported plate are shown in Figs 11, 12 and Figs 13, 14 for the case of a free hole and a plugged hole, respectively. In order to assess the effect of various parameters in the range of small as well as large deflection, the linear response obtained by the present method is given in Table 4 for static loadings.

It can be noted from Table 4 that for linear small deflection response, the influence of the orthotropic parameter β is much larger for plates with a free hole than for plates with a plugged hole, for both clamped and simply supported edge conditions. The effect of β is more pronounced for the simply supported plates than for the clamped plates. The taper ratio α has very large effect on deflection in all cases. Typical nonlinear stiffening followed by linearity in the deflection response is observed in Fig. 2 and Figs 4–14. The effect of β and α decreases with deflection. The effect of taper ratio decreases with deflection since bending action (dependent on h^3) predominates for small deflections, whereas membrane action (dependent on h) predominates for large deflections. It can be seen from Figs 11–14 that for large deflection, the taper ratio α has lesser effect for the simply supported plate than the clamped plate. It is evident from Figs 7–10 and Figs 13, 14 that the effect of orthotropic parameter β is much less for plates with plugged holes than for those with free holes, and its effect decreases further with annular ratio.

It may be concluded that a simple method can be used to obtain approximate value of the maximum dynamic response to step loads from the static response. The accuracy of the approximate response is sufficient for engineering applications. The new static and transient results presented herein for orthotropic annular plates of variable thicknesses with and without a plugged hole subjected to uniformly distributed and ring loads may be of some interest in the design of fibre-reinforced composite plates.

REFERENCES

1. S. D. N. Murthy and A. N. Sherbourne, Nonlinear bending of elastic plates of variable profile. *J. Engng Mech. Div., Proc. ASCE* **100**, 251–265 (1974).
2. G. J. Turvey, Large deflection of tapered annular plates by dynamic relaxation. *J. Engng Mech. Div., Proc. ASCE* **104**, 351–366 (1978).

3. J. T. Tielking, Axisymmetric bending of annular plates. *J. Appl. Mech.* **45**, 834–838 (1978).
4. J. N. Reddy and C. L. Huang, Nonlinear axisymmetric bending of annular plates with varying thickness. *Int. J. Solids Struct.* **17**, 811–825 (1981).
5. J. N. Reddy and C. L. Huang, Large amplitude free vibrations of annular plates of varying thickness. *J. Sound Vib.* 387–396 (1981).
6. Y. Nath and R. K. Jain, Nonlinear dynamic analysis of orthotropic annular plates resting on elastic foundations. *Earthquake Engng and Struct. Dynamics* **11**, 785–796 (1983).
7. J. V. Villadsen and M. L. Michelsen, *Solution of Differential Equation Models by Polynomial Approximation*. Prentice-Hall, Englewood Cliffs, New Jersey (1978).
8. K. J. Bathe and E. L. Wilson, *Numerical Methods in Finite Element Analysis*. Prentice-Hall, Englewood Cliffs, New Jersey (1976).